

10-12-2018

Computational modeling and functional characterization of a GgChi: A class III chitinase from corms of *Gladiolus grandiflorus*

Maria Rafiq

Bahauddin Zakariya University

Ashiq Hussain

Technical University of Munich

Kausar Hussain Shah

Bahauddin Zakariya University

Qamar Saeed

Bahauddin Zakariya University

Muhammad Umair Sial

Chinese Academy of Agricultural Sciences

See next page for additional authors

Follow this and additional works at: <https://digitalcommons.unl.edu/foodsciefacpub>

Part of the [Food Science Commons](#)

Rafiq, Maria; Hussain, Ashiq; Shah, Kausar Hussain; Saeed, Qamar; Sial, Muhammad Umair; Ali, Zahid; Buck, Friedrich; Goodman, Richard E.; Khaliq, Binish; Ishaq, Uzma; Baig, Mirza Ahsen; Munawar, Aisha; Mahmood, Seema; and Akrem, Ahmed, "Computational modeling and functional characterization of a GgChi: A class III chitinase from corms of *Gladiolus grandiflorus*" (2018). *Faculty Publications in Food Science and Technology*. 302.
<https://digitalcommons.unl.edu/foodsciefacpub/302>

This Article is brought to you for free and open access by the Food Science and Technology Department at DigitalCommons@University of Nebraska - Lincoln. It has been accepted for inclusion in Faculty Publications in Food Science and Technology by an authorized administrator of DigitalCommons@University of Nebraska - Lincoln.

Authors

Maria Rafiq, Ashiq Hussain, Kausar Hussain Shah, Qamar Saeed, Muhammad Umair Sial, Zahid Ali, Friedrich Buck, Richard E. Goodman, Binish Khaliq, Uzma Ishaq, Mirza Ahsen Baig, Aisha Munawar, Seema Mahmood, and Ahmed Akrem



Available online at www.sciencedirect.com

ScienceDirect

journal homepage: <http://www.kjms-online.com>



Original Article

Computational modeling and functional characterization of a GgChi: A class III chitinase from corms of *Gladiolus grandiflorus*



Maria Rafiq ^a, Ashiq Hussain ^b, Kausar Hussain Shah ^a, Qamar Saeed ^c, Muhammad Umair Sial ^d, Zahid Ali ^e, Friedrich Buck ^f, Richard E. Goodman ^g, Binish Khaliq ^a, Uzma Ishaq ^h, Mirza Ahsen Baig ^a, Aisha Munawar ⁱ, Seema Mahmood ^a, Ahmed Akrem ^{a,*}

^a Botany Division, Institute of Pure and Applied Biology, Bahauddin Zakariya University, Multan, Pakistan

^b TUM School of Life Sciences Weihenstephan, Technical University of Munich, Germany

^c Department of Entomology, Bahauddin Zakariya University, Multan, Pakistan

^d Institute of Plant Protection, Chinese Academy of Agricultural Sciences, Beijing, PR China

^e Department of Biosciences, COMSATS University Islamabad, Park Road, Islamabad, Pakistan

^f Institute of Clinical Chemistry, University Medical Centre Hamburg-Eppendorf, Hamburg, Germany

^g Food Allergy Research and Resource Program, Department of Food Science & Technology, University of Nebraska–Lincoln, Lincoln, USA

^h Department of Botany, The Women University, Multan, Pakistan

ⁱ Department of Chemistry, Faculty of Natural Sciences, Humanities & Islamic Studies, University of Engineering and Technology, Lahore, Pakistan

Received 5 March 2018; accepted 7 August 2018

Available online 12 October 2018

KEYWORDS

Gladiolus grandiflorus;
Endochitinase;
TIM barrel;
Antibacterial;
Antifungal

Abstract The present study describes the predicted model and functional characterization of an endochitinase (30 kDa) from corms of *Gladiolus grandiflorus*. ESI-QTOF-MS generated peptide showed 96% sequence homology with family 18, Class III acidic endochitinase of *Gladiolus gandavensis*. Purified *G. grandiflorus* chitinase (GgChi) hydrolyzed 4-methylumbelliferyl β -D-N,N',N''-triacetylchitotriose substrate showing specific endochitinase activity. Since no structural details of GgChi were available in the Protein Data Bank (PDB), a homology model was predicted using the coordinate information of *Crocus vernus* chitinase (PDB ID: 3SIM). Ramachandran plot indicated 84.5% in most favored region, 14.8% in additional and 0.6% in

Conflicts of interest: All authors declare no conflicts of interest.

* Corresponding author. Institute of Pure and Applied Biology, Bahauddin Zakariya University, 60800 Multan, Pakistan
E-mail address: ahmedakrem@bzu.edu.pk (A. Akrem).

<https://doi.org/10.1016/j.kjms.2018.08.003>

1607-551X/Copyright © 2018, Kaohsiung Medical University. Published by Elsevier Taiwan LLC. This is an open access article under the CC BY-NC-ND license (<http://creativecommons.org/licenses/by-nc-nd/4.0/>).

generously allowed region while no residue in disallowed region. The predicted structure indicated a highly conserved (β/α)₈ (TIM barrel) structure similar to the family 18, class III chitinases. The GgChi also showed sequence and structural homologies with other active chitinases. The GgChi (50 $\mu\text{g}/\text{disc}$) showed no antibacterial activity, but did provide mild growth inhibition of phytopathogenic fungus *Fusarium oxysporum* at a concentration of 500 $\mu\text{g}/\text{well}$. Similarly, insect toxicity bioassays of GgChi (50 μg) against nymphs of *Bemisia tabaci* showed 14% reduction in adult emergence and 14% increase in mortality rate in comparison to control values. The GgChi (1.5 mg) protein showed significant reduction in a population of flour beetle (*Tribolium castaneum*) after 35 days, but lower reactivity against rice weevil (*Sitophilus oryzae*). The results of this study provide detailed insight on functional characterization of a family 18 class III acidic plant endochitinase.

Copyright © 2018, Kaohsiung Medical University. Published by Elsevier Taiwan LLC. This is an open access article under the CC BY-NC-ND license (<http://creativecommons.org/licenses/by-nc-nd/4.0/>).

Introduction

Chitin is a linear polymer of β -1,4-N-acetylglucosamine (GlcNAc). It is the second most abundant biopolymer on the planet after cellulose [1]. Chitin provides structural strength to a wide variety of organisms and is important for self-defense [2]. It is found in the fungal cell wall, exoskeleton of insects and in the internal structures of other vertebrates [3]. Chitinases are hydrolytic enzymes that break down glycoside bonds in chitin. Chitinases play an important role in the cell division and morphogenesis of the organism and as pathogenesis related proteins that inhibit the growth of pathogenic fungi in plants [4]. Chitinase expression in plants is driven by the NPR1 gene and utilizes the salicylic acid pathway to provide fungal resistance as well as stops the insect attack [5]. Chitinases are diverse proteins that vary in their structure, localization, and substrate specificity, yet all catalyze the hydrolytic cleavage of β -1,4-glycoside bond of chitin [6]. Additionally, these enzymes also hydrolyze the deacetylated form of chitin, referred to as chitosan [7]. The plant chitinases are divided into many classes i.e., I, II, III, IV, V, VI and VII [8]. However, in the glycosyl hydrolase classification system, these chitinases are grouped into two families i.e. GH-18 and GH-19 [9]. Classes I, II, IV, VI and VII are found only in plants corresponding to the GH-19 family, whereas classes III and V belong to the GH-18 family as per the carbohydrate-active enzyme (CAZy) database [10]. Family 18 chitinases utilize substrate-assisted double-displacement mechanism which involves the configuration retention of the anomeric carbon by producing β -anomers [11].

Iridaceae comprised of traditional medicinal plants as rich source of secondary metabolites [12]. In natural circumstances, the seeds and corms are frequently attacked by various pathogens including viruses, bacteria, fungi and nematodes [13]. Various chitinase enzymes have received attention due to their broad applications in biotechnology, medicine, waste management and other industries as well as in agriculture for biocontrol of phytopathogenic fungi and harmful insects [14]. In this study, a 30 kDa chitinase (GgChi) has been purified and characterized from corms of *Gladiolus grandiflorus* plant. A three dimensional model was generated using online server Phyre² [15]. Thorough functional

characterization of GgChi is also presented against different microbial and insect pathogens.

Materials and methods

A 30 kDa family 18, class III endochitinase was characterized from corms of *G. grandiflorus*. All reagents used in experiments were of analytical grade.

Protein quantifications

Total water soluble proteins were quantified by Bradford assay [16] using Bovine Serum Albumin as standard. The absorbance at 595 nm was checked using double beam UV/VIS spectrophotometer (BMS, S/N-204573, USA).

Protein electrophoresis

The isolated protein samples alongwith unstained protein marker (Catalog No. 623112375001730) were resolved on 12% polyacrylamide gels by following standard procedure of SDS-PAGE [17] and using E-VS10-SYS, omni PAGE mini-System (Germany). The gels were stained with Coomassie Brilliant Blue R-250 (Sigma Aldrich) for visualizing the proteins.

Protein purification

Corms of *G. grandiflorus* were washed using distilled water before peeling the outer skin. The soft inner tissue was frozen and ground using liquid nitrogen-chilled mortar and pestle. Finely ground plant material was suspended in 50 mM phosphate buffer of pH 6.0 with 1 mM PMSF, Protease inhibitor cocktail (Sigma, S8820) and 5% glycerol. Proteins were extracted by continuously stirring for 3 h. The plant extracts were clarified by centrifugation at 12 000 rpm for 10 min at 4 °C in a Centurion, K241R centrifuge. The supernatant was passed through a filter paper (8 μm pore size) and the protein was purified from the filtrate.

Crude extract was subjected to 60% ammonium sulfate precipitation and protein precipitates were recovered by centrifuging at 5000 rpm for 5 min. The pellet was re-suspended and dialyzed (MWCO 3.5 kDa) overnight with 50 mM acetate buffer (pH 5.0). The transparent

supernatant was loaded on a CM Sepharose Fast Flow column that was pre-equilibrated with buffer A (50 mM acetate; pH 5.0). The adsorbed protein was eluted with buffer B by using a linear gradient of 1.0 M NaCl. The partially purified, desalted chitinase was loaded on a Superdex G-200 10/300 GL column for further purification. The protein was eluted using 50 mM acetate buffer containing 200 mM NaCl. Eluted fractions were resolved on 12% SDS-PAGE and the fractions with maximum protein concentrations and greatest purity were pooled together and salt was removed again by dialysis. The purified enzyme was used for further characterization studies.

ESI-QTOF-MS analysis for chitinase identification

Protein bands were cut out and reduced with DTT (10 mM, 56 °C, 30 min). The cysteine residues were modified with iodoacetamide (55 mM, ambient temperature, 20 min in the dark) and the proteins were digested in-gel with trypsin (5 ng trypsin/ μ l; sequencing grade modified trypsin, Promega, Madison, USA) in 50 mM NH_4HCO_3 (37 °C, 16 h). After digestion, the gel pieces were repeatedly extracted by 50% acetonitrile/5% formic acid solution and the combined extracts were dried down in a vacuum concentrator. The lyophilized powder; re-dissolved in 5% methanol/5% formic acid, was desalted on a C18 μ ZipTip[®] (Millipore, Billerica, USA) and eluted with 1 μ l 60% methanol/5% formic acid to be analyzed by nano-electrospray mass spectrometry [18] in a QTOF II instrument (Micromass, Manchester, UK). MS/MS spectra; obtained by collision induced fragmentation after manual precursor selection, were evaluated manually.

Chitinase assay kit

The chitinase activity was performed using a chitinase assay kit (Fluorimetric, CS1030; Sigma) provided with three substrates i.e., 4-methylumbelliferyl *N*-acetyl- β -D-glucosaminide (4MUG) for exochitinase detection and chitobiosidase activity; 4-methylumbelliferyl β -D-*N,N'*-diacetylchitobioside (4MUC) hydrate for exochitinase detection and β -*N*-acetylglucosaminidase activity and 4-methylumbelliferyl β -D-*N,N',N''*-triacetylchitotriose (4MUT) for detection of endochitinase activity for the elucidation of substrate specificity. The Fluorimetric absorbance was recorded applying the GENios Instrument XFlour4, version 4.51 (Tecan, Austria). Enzyme units were calculated by preparing the serial dilutions of 4MU ranging from 10 ng/assay standard to 1000 ng/assay standard dilutions. One Unit of GgChi was defined as 1 μ mole of 4MU liberated from appropriate substrate per minute at pH 5.0 and 37 °C. The activity was measured using linear regression analysis forming a standard curve of the fluorescence readings of 5 standard solutions including blank.

Homology modeling and structure prediction

Multiple sequence alignment was performed using ClustalW2 at EMBL-EBI (<http://www.ebi.ac.uk/Tools/msa/clustalw2/>) and Box Shade server (http://www.ch.embnet.org/software/BOX_form.html). The FASTA sequences of different plant chitinases were obtained

from the UniProtKB (www.uniprot.org) database. The final multiple sequence alignment was edited using structural information and secondary structure analysis which was carried out in the PSIPRED (<http://bioinf.cs.ucl.ac.uk/psipred/>) server. For prediction of three dimensional structure through homology modeling, the homologous proteins were identified based on identity matches by BLASTP from the Protein Data Bank (PDB) database (<http://www.rcsb.org/pdb/home/home.do>) and the templates with maximum quality were selected for the prediction of model. The sequence prediction for GgChi was conceded by using Phyre² (Protein Homology/AnalogY Recognition Engine), an automatic fold recognition server for calculating the structure and function of protein sequence, www.sbg.bio.ic.ac.uk/phyre2. The Phyre² server uses an archive of known protein structures from the Structural Classification of Proteins (SCOP) database [19] amplified with newer depositions in the Protein Data Bank (PDB) [20]. The sequence of each of these known structures was scanned against a non-redundant sequence database and a profile was constructed and deposited in the 'fold library'. The known and predicted secondary structures of these proteins were stored in the fold library. The unknown sequence (query) was similarly scanned against the non-redundant sequence database and a profile was constructed. Five iterations of PSI-Blast were used to gather both the close and the remote sequence homologs of the 'query' PROCHECK [21] was used to analyze the Ramachandran plot, peptide bond planarity, main chain hydrogen bond energy and overall G-factors. The $C\alpha$ root mean square deviation (r.m.s.d) values between the predicted model and comparing templates were calculated from iPBA web server (http://www.dsimb.inserm.fr/dsimb_tools/ipba/index.php). The software Chimera [22] was used for the preparation and presentation of the GgChi cartoon models.

Antibacterial assay

The antibacterial potential of GgChi was evaluated against different bacterial strains using a modified Kirby–Bauer susceptibility test [23]. Commercial antibiotic discs (Amoxicillin/Clavulanic acid 30 μ g; Oxoid CT0223B) were used as positive controls and a disc wetted with sterile water was used as a negative control (mock). Six bacterial strains (*Staphylococcus aureus*, *Escherichia coli*, *Bacillus subtilis*, *Xanthomonas oryzae*, *Pseudomonas syringae* and *Pseudomonas aeruginosa*) were cultured in LB agar plates by applying active bacterial culture ($\sim 10^6$ cells/ml) over the surface by sterile cotton swab sticks. Sterilized discs (6 mm diameter; Whatman filter paper) were soaked in 25 and 50 μ g concentrations of GgChi. All the discs were placed on equidistance from center of the agar surface. The experiment was repeated in triplicate and data was recorded after 8 h.

Antifungal assay

Mature *Fusarium oxysporum* conidia were prepared from fungal cultures; grown in PDA plates (at 28 °C), by addition of 15 ml pre-chilled distilled water followed by incubation

for 2–4 h at 4 °C. The fungal culture was then gently stirred for 1 min with a sterile loop before pouring solution through three-layered sterile cheese cloth into a sterile falcon tube. Conidia were counted at 400× magnification using hemocytometer (NeubauerHausser Bright-Line; Catalog No. 3100) and adjusted to a standard concentration of 2×10^4 cells ml⁻¹ in 1 ml of 0.15 M saline solution. Inhibition of fungal growth was tested by incubating conidia at 28 °C in 200 µl 96 well microtitre plates in the presence of 50, 100, 200, 300, 400 and 500 µg/well of GgChi protein concentrations. Saline solution alone was used as mock (control). The optical density of the samples was measured at 600 nm at 0, 24 and 48 h post-incubation. Experiments were carried out in triplicate and the mean values, standard errors and coefficients of variation were calculated. The readings were plotted in MS-Excel to reveal growth pattern of conidia.

Insect toxicity bioassays

Nymphs of *Bemisia tabaci* (Silver leaf whitefly) were reared and the toxicity assays were performed at National Agricultural Research Center (NARC), Islamabad, Pakistan. The insects were collected from cotton fields, fed on artificial diet and cultured inside air conditioned insectaries at 25 ± 2 °C, relative humidity (r.h.) of $65 \pm 5\%$ using a photoperiod of 16 h light and 8 h dark time. Fresh whitefly nymphs were used for toxicity bioassays under the same environmental conditions. The nymphs of *B. tabaci* were placed in petri dishes containing excised cotton leaf discs (4 cm diameter) which were impregnated with 20 µl (50 µg) protein samples and water as control. Two independent experiments were run targeting adult emergence from nymphs in one experiment and mortality rate in second experiment. Both experiments were conducted in five replicates with single constant protein dose (50 µg) which was applied once in the start of experiment and data was recorded once after seven days. In first experiment, nymphs that transformed to adults were taken as alive for proper scoring.

Stored product insect pests

Heterogeneous populations of *Tribolium castaneum* and *Sitophilus oryzae* were collected from local grocery market of Multan. Cultures were controlled under laboratory temperature of 25 ± 2 °C and 65 ± 5 r.h. Insecticidal activities of GgChi were tested on adults of *T. castaneum* and *S. oryzae* exposed to one of three doses (1.5, 1.0 and 0.5 mg/ml) as a food admixture [24].

Tribolium castaneum

Protein doses were prepared in 100 ml buffer and mixed with 150 g wheat flour, pre-chilled to 4 °C. Control meal was prepared with wheat flour in buffer. Treated flour and control samples were allowed to dry in the dark for 10 days and then ground to a powder for feeding. Five replicates of 30 g flour were used for each dose of GgChi and control. Chitinase impacts on insect progeny were determined 35 days later [25]. Insects were placed in glass jars of appropriate volume with 5 pairs of *T. castaneum* adults per

replicate. Adults were removed after ten days and glass jars kept undisturbed for 35 days before counting progeny. Average counts were compared with controls to determine efficacy against *T. castaneum*.

Sitophilus oryzae

Protein doses were prepared in 50 ml buffer solution to coat 100 g rice kernels and were air dried before use. Protein and control samples were replicated five times in glass jars of appropriate volume and 20 randomly selected individuals [26] and the adults were removed after 10 days. The impact of GgChi was determined after an additional period of 35 days and then progeny was counted and compared to control sample.

Statistical analysis

The insect-toxin protein bioassay data were analyzed in one way ANOVA through "Statistix 8.1" and means were separated by Tukey-LSD test with significance level of 0.05 [27]. Standard errors of each concentration were also computed through Microsoft Excel 2010.

Results

Chitinase purification and identification by ESI-QTOF mass spectrometry

A purified 30 kDa GgChi was observed on SDS-PAGE under both non-reducing and reducing conditions after optimization of column chromatography (Fig. 1). The different concentrations (w/v) of GgChi were measured by Bradford reagent and were used to perform different bioassays. A GH-18 family, class III chitinase (GgChi) was identified by ESI-QTOF-MS which provided seven fragments of GgChi enzyme comprising a protein of 176 residues out of 275 amino acids approximately and was compared to known sequences of homologous chitinases (Fig. 2). The tryptic peptide NLFVEYIGSQFTGLKFTDVPINPR was found with N-terminal mass increment of 57 Da. This N-terminal modification is most likely due to the treatment of the protein with iodoacetamide before digestion and indicates that this peptide represents the N-terminus of the mature protein. Based on the amino acid sequence of this peptide, a protein BLAST search was run using the UniProtKB database which showed higher identities with previously reported family 18, class III acidic endochitinases as shown in Table 1. Multiple sequence alignment analysis revealed that the protein is composed of a glycoside hydrolase super family domain (residues: 49–171). The conserved regions RI and RII (marked by red boundaries) are of special interest in class-III chitinases [28]. The conserved region RI contained specific chitin binding motif SXGG (80–83) while the conserved region RII contained catalytic site of class-III chitinases [29]. The presence of catalytic domain DXDXE (122–126) further confirmed the protein as a glycosyl hydrolase family 18 type chitinase. Narbonin protein of *Vicia narbonensis* was also aligned to show the mutation in the catalytic site replacing second aspartate with histidine

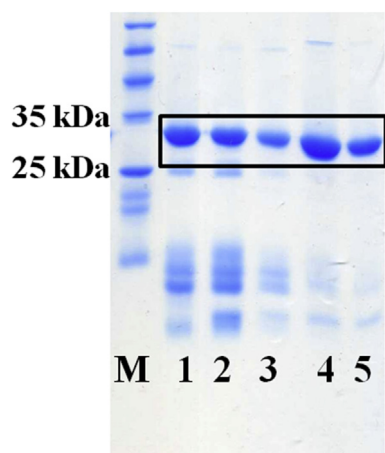


Figure 1. SDS-PAGE is showing the stepwise purification of 30 kDa GgChi (black square) from corms of *Gladiolus grandiflorus*. Lane M is the pre-stained protein ladder (Pierce™ Unstained Protein MW Marker; Catalog No: 26610) with 25 and 35 kDa bands highlighted. Lanes 1 & 2 are showing impure crude extracts. Lane 3 is showing the result of eluted protein from CM-Sepharose column while lanes 4 & 5 are showing highly purified fractions after gel filtration chromatography.

(DXHXE) and resulting in ultimate loss of chitinase activity (Fig. 2). A single cysteine was found in three sequences of *G. grandiflorus*, *Gladiolus gandavensis* and *Crocus vernus* chitinases. However, this Cysteine (Cys₁₃₉) was replaced with Leucine (Leu₁₃₉) in narbonin protein as highlighted by yellow squares in Fig. 2. Hence no disulfide linkage was found in all the structures. A high sequence identity was experienced between class III chitinases of *G. grandiflorus* and *G. gandavensis*. Nevertheless, a total of nine amino acid variations have been found scattered all over the sequence as highlighted with yellow background (Fig. 2). This small percentage of sequence dissimilarity is indicative of two very closely related isoforms of acidic chitinases, probably originated from slightly different evolutionary pathways of two species. Similarly, the variable amino acids; highlighted with red background, might be due to the errors in data interpretation and might need further confirmation. Similarly, amino acid Asp₁₃₄ of *G. gandavensis* (highlighted in green background) differs from closely aligned sequences of *C. vernus* and *G. grandiflorus*. Trp₅₅ and Trp₂₅₂ appear to be the aromatic side chains involved in binding sugar residues [8]. These residues are conserved in family 18 chitinases and are shown by filled inverted triangles.

Chitinase assay

The hydrolytic product 4-methylumbelliferone (4MU) was liberated as a result of enzymatic action of GgChi on 4-methylumbelliferyl β -D-N,N',N'-triacetylchitotriose (4MUT) substrate and was measured fluorimetrically in an alkaline pH with excitation at 360 nm and emission at 450 nm. GgChi provided significant endochitinase activity (84 U/mg) by hydrolyzing the 4-methylumbelliferyl β -D-N,N',N'-triacetylchitotriose substrate in comparison to other

substrates (Fig. 3). The chitinase of *Trichoderma viride*; used as positive control, showed relatively high exochitinase and β -N-acetylglucosaminidase activity.

GgChi homology modeling

The information about the conserved domains of GgChi was retrieved from InterPro protein family's database. For the predicted model calculation of the GgChi, BLAST found several homologous chitinases with known 3-D structures in Protein Data Bank (PDB). The matched proteins were checked carefully regarding the sequence similarities to GgChi in terms of finding the proper reference model (Table 2). Finally, the coordinate information (PDB ID: 3SIM) of *C. vernus* chitinase (CVC); showing 49% sequence identity and 54% sequence similarity with fragmented MS data of GgChi, was selected for the calculation of GgChi hypothetical model. It was found that GgChi sequence has high similarity with 100% confidence and 99% coverage to the crystallographic structure of 3SIM, which is class III family 18 chitinase from *C. vernus*. Out of total 274, 270 residues (99% of query sequence) have been modeled with 100% confidence by the single highest scoring template. The predicted three dimensional model of GgChi (Fig. 4A) was checked by Ramachandran plot. The results of the Ramachandran plot produced by PROCHECK showed a homology model with good stereo chemical quality, which was supported by 84.0% residues in most favored regions, 14.8% in additional allowed regions and 0.6% in generously allowed regions. The overall G-factors produced by PROCHECK were 0.03, also suggesting a homology model of good quality. The structure of GgChi was compared with other family GH-18 proteins including *C. vernus* chitinase and narbonin protein of *V. narbonensis* (Fig. 4B). The GgChi predicted model was superimposed to 3SIM and 1NAR with α r.m.s.d values of 0.22 and 1.35 Å respectively between equivalent atom pairs. A lower r.m.s.d value was observed probably due to high sequence and structural homology among the three structures comprising of highly conserved TIM barrel fold.

Antibacterial activity of GgChi

The purified GgChi was studied in vitro for growth inhibition activity against six types of bacterial species. No antibacterial activity was observed for the two concentrations (25 and 50 μ g) of GgChi protein (Fig. 5A–F). Significant inhibition zones were observed for the commercial antibiotic discs, but no such inhibition zones were observed for the enzyme itself.

Antifungal activity of GgChi

A range of enzyme concentrations were used to determine antifungal activity. A mild antifungal activity was observed for the purified chitinase against phytopathogenic fungus *F. oxysporum*. About 50% fungal growth was inhibited by chitinase at concentration of 500 μ g/well (Fig. 6).

Insecticidal toxicity

The insecticidal effect of GgChi was tested against nymphs of *B. tabaci* (Silver leaf whitefly) by analyzing their adult

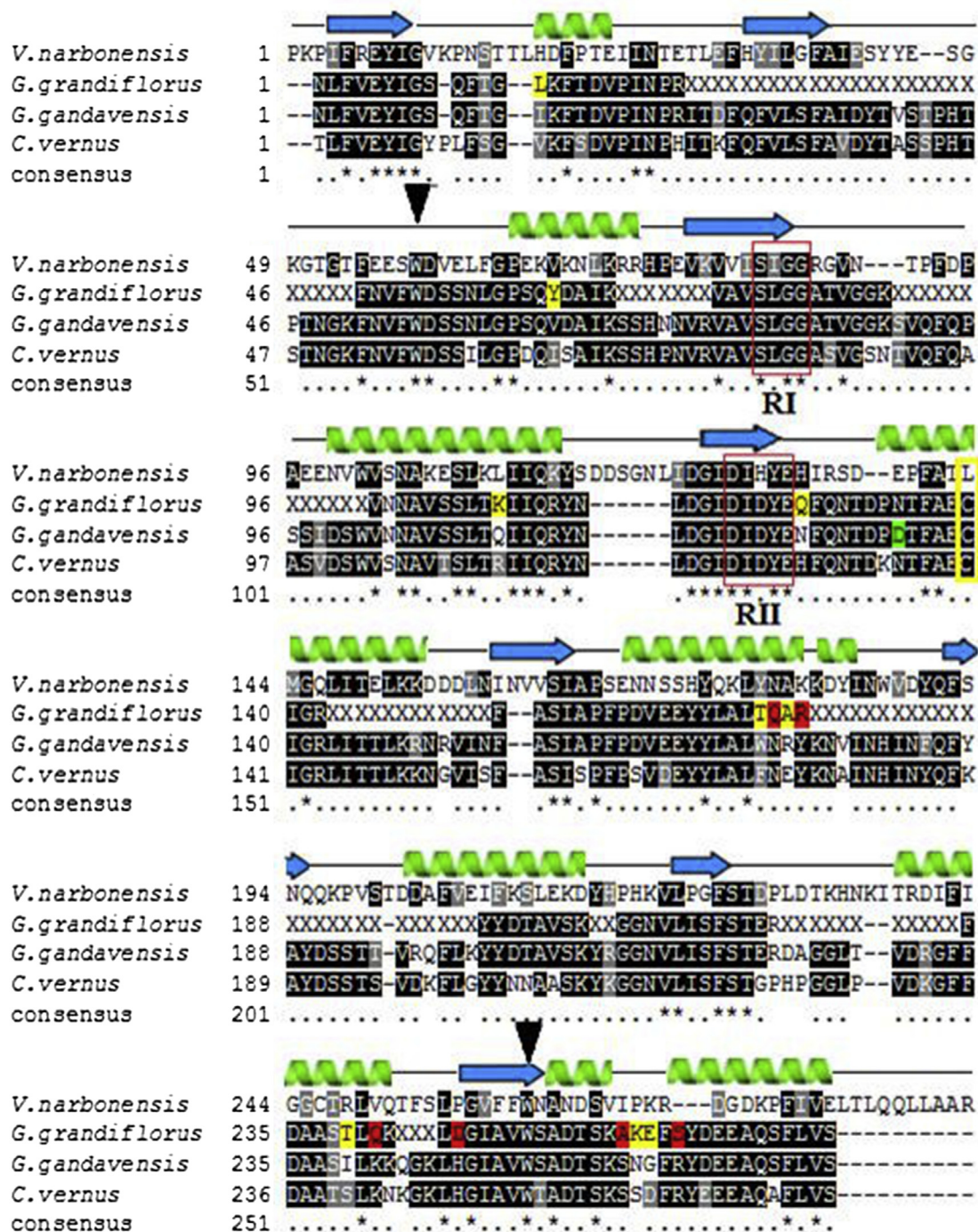


Figure 2. Sequence alignment of GgChi with other homologous plant chitinases. Black background is showing conserved regions. The conserved DXDXE and SXGG motifs; observed in all family 18 chitinases, are highlighted by red boundary. Secondary structures of GgChi (α -helix and β -sheet) were indicated at the top of sequence alignment by using Phyre² and PSIPRED. Dashes indicate gaps and * indicates exactly identical residues among all chitinases.

emergence and mortality on cotton leaves in response to GgChi treatment (Table 3). The GgChi protein showed a mild insecticidal activity against nymphs of *B. tabaci*. GgChi concentration of 50 μ g per leaf disc produced 14% reduction in adult emergence and 14% increase in mortality rate, which is moderately higher than control.

Stored product insect pests

Efficacy of GgChi protein was tested against adult and progeny populations of *T. castaneum* and *S. oryzae* pests (Fig. 7). Minimum *T. castaneum* progeny was observed after 35 days of exposure at highest dose of 1.5 mg/ml (4.2 ± 0.8

Table 1 *G. grandiflorus* chitinase (GgChi) showed maximum identity (96%) with *Gladiolus gandavensis* family 18, class III endochitinase. Similarly, high homologies were observed with endochitinases of other plant species including *Oryza sativa*, *Zea mays* and *Crocus vernus*.

Plants	Chitinases	Sequence	Homology (%)	References
<i>G. grandiflorus</i>	GgChi	NLFVEYIGSQFTGLKFTDVPINPR	100	This paper
<i>G. gandavensis</i>	Chitinase a	NLFVEYIGSQFTGKFTDVPINPR	96	Q7M1R1
<i>O. sativa</i>	Class III chitinase	LFREYIGAQFTGVRFSVDPINP	77	Q8S870
<i>Z. mays</i>	Chitinase 2	NLFRDYIGAIFNGVKFTDVPINPR	75	B6U7J7
<i>C. vernus</i>	Family 18 Chitinase	LFVEYIGYPLFSGVKFSDVPINP	74	G1K3S3

adults) at $P < 0.05$. Likewise, 1.0 and 0.5 mg/ml doses almost equally presented the effectiveness i.e. 8.2 ± 0.7 adults and 8.8 ± 0.2 adults, respectively compared to the control group (19.4 ± 1.3 adults). The GgChi was somewhat less effective against *S. oryzae* with a reduction of approximately 70% compared to the control group at the highest dose. Minimal progeny of rice weevil was observed at highest dose on 1.5 mg/ml (17 ± 2.9 adults) at $P < 0.05$, whereas, doses of 1.0 mg/ml and 0.5 mg/ml were similar as 32.4 ± 3.1 and 35.2 ± 3.1 adults, respectively. All doses resulted in reduction of new insects compared to the control group (46.6 ± 1.6 adults). An increased dose above the current levels tested would be expected to improve efficacy.

Discussion

Defining the structure and function of a protein is the epicenter of many aspects of modern biology. New profile–profile matching algorithms have improved the practice of protein structure prediction in recent years. Three dimensional structures of proteins are more informative than their linear polypeptide sequences because different patterns may be formed and interactions might exist among distant residues forming specific recognizable motifs. Using such algorithms, we have reliably detected the protein structure of GgChi which is very similar to family 18 chitinase from *C. vernus* (PDB ID: 3SIM) that was selected as template due to better query coverage, high

sequence similarity and smaller E-value. The Ramachandran plot indicated a better and accurate predicted model of GgChi protein.

Higher similarity between these two proteins contributed to the assumption that these proteins perform same function in both plants. Chimera was used for the depiction of the overall molecular structure of GgChi (Fig. 4A) which proposed classical TIM-barrel structure of the enzyme comprising of typical $(\beta\alpha)_8$ fold [30]. The secondary structure comprised of a $(\beta/\alpha)_8$ domain which lined the binding site and is made up of 8 core parallel β sheets (Residues (β_1) 2–7, (β_2) 29–38, (β_3) 74–83, (β_4) 119–24, (β_5) 155–159, (β_6) 181–184, (β_7) 213–220, (β_8) 248–252 and 8 α -helices (Residues (α_1) 15–19, (α_2) 61–72, (α) 97–116, (α_4) 132–150, (α_5) 165–175, (α_6) 194–209, (α_7) 232–243 and (α_8) 262–274) (Fig. 2). The outer surface of GgChi is surrounded by hydrophilic amino acids mainly by aspartate, asparagine, lysine and two major polar amino acids i.e., serine and threonine. The inside β -barrel is lined mainly with hydrophobic amino acids like valine, isoleucine, phenyl alanine and alanine. Few glycine residues were also observed lying on the sides of this barrel. Three tyrosine residues were also found in close proximity of this barrel with only one tryptophan hanging inside the cavity. Structural comparisons were made between TIM barrel chitinases of 1NAR and 3SIM (Fig. 4B). This signature motif (Asp122–Glu126) is located in the loop between β_4 strand and α_4 helix [31]. Glu126 is the catalytic acid/base while aspartic acid residue Asp124 is critical for stabilizing the enzyme–substrate intermediate and Asp122 appears to be crucial for keeping Asp124 protonated in GgChi active site [8].

Functional characterization of GgChi was performed by antibacterial, antifungal and insecticidal activity assays. Altogether, GgChi did not provide any significant microbial growth inhibition rather a mild or no activity was observed

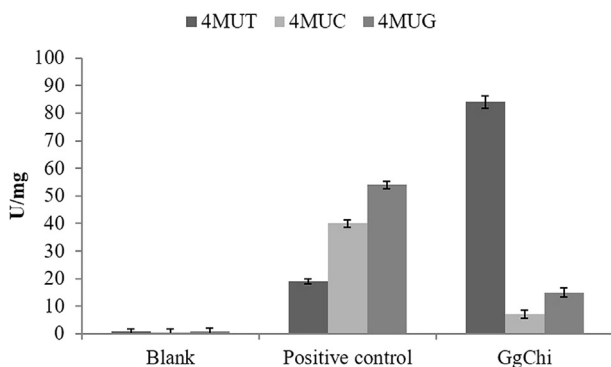


Figure 3. Endochitinase activity of GgChi was assessed and calculated by chitinase assay kit. GgChi showed significant activity (84 U/mg) by hydrolyzing the 4-methylumbelliferyl β -D-N,N',N''-triacetylchitotriose (4MUT) substrate in comparison to other substrates.

Table 2 PDB entries of plant chitinases showing sequence homologies with GgChi sequence. However, the coordinate information of *C. vernus* chitinase (PDB ID: 3SIM) was used later on for the calculation of the predicted model.

Sr. No.	PDB ID	Botanical name	Entry year	%age Identity
1	3SIM	<i>Crocus vernus</i>	2011	49
2	2HVM	<i>Hevea brasiliensis</i>	1997	16
3	1CNV	<i>Canavalia ensiformis</i>	1996	16
4	1NAR	<i>Vicia narbonensis</i>	1994	33

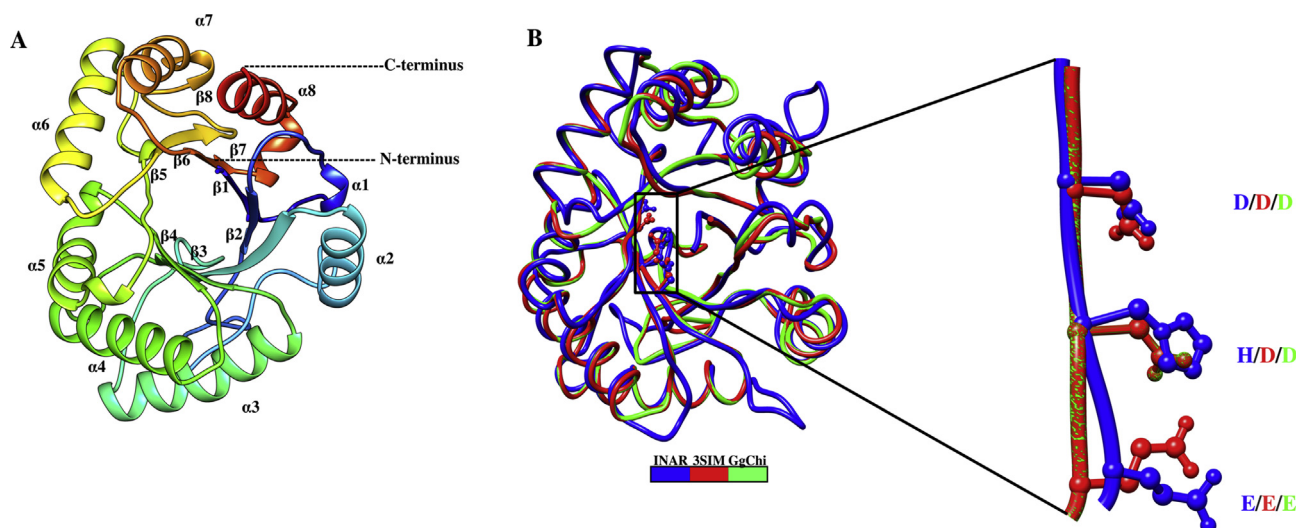


Figure 4. Overall structure showing a stereo view of the native GgChi. (A) Three-dimensional structure was predicted and is shown as ribbon diagram. The secondary structure elements are labeled in α -helices and β -sheets. (B) Catalytic motif is highlighted by comparing the three TIM barrel structures (PDB ID: 3SIM, 1NAR and hypothetical GgChi model).

during the in vitro bioassays. In a previous study, it was reported that the PL Chi-A class III acidic chitinase from pineapple leaves had chitinolytic activity toward soluble chitin but did not exhibit antifungal activity. The cleavage pattern of N-acetyl chitooligosaccharides by PL CHI-A might indirectly affect the invasion of pathogens, as by elicitor producing, or may have other functions [32]. In plants, there are 2 classes of chitinases, basic or acidic chitinases,

targeting different parts of the cell and are differentially regulated [33]. There are examples of chitinases that are not primarily associated with chitin degradation even though they are able to display a chitinolytic activity [34]. Acidic and basic chitinases have been reported *Cicer arietinum* cell-suspension cultures, but only the basic chitinase possessed antifungal activity while acidic class III chitinase was devoid of fungicidal activity [35]. Among the class III

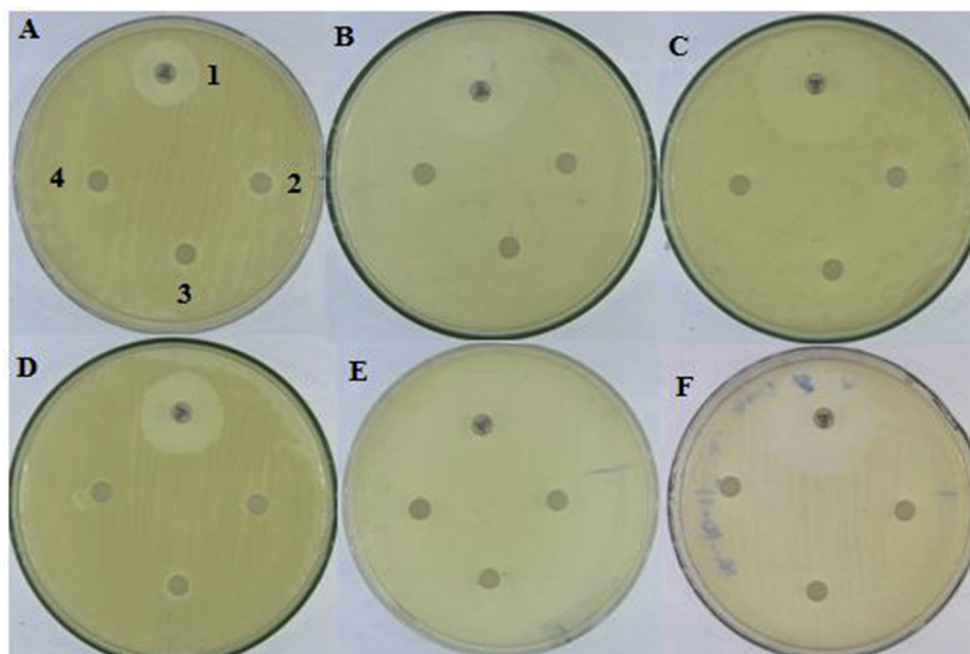


Figure 5. Antibacterial activity of GgChi against different pathogenic bacteria. A, *Bacillus subtilis*; B, *Escherichia coli*; C, *Pseudomonas syringae*; D, *Staphylococcus aureus*; E, *Xanthomonas oryzae*; F, *Pseudomonas aeruginosa*. Label 1 indicates the amoxicillin disc as positive control, 2 indicates the water as negative control, 3 indicates the 50 μ g treatment and 4 indicates the 25 μ g treatment of GgChi protein respectively. All the six plates have been designed in the identical fashion regarding the placement and labeling of discs.

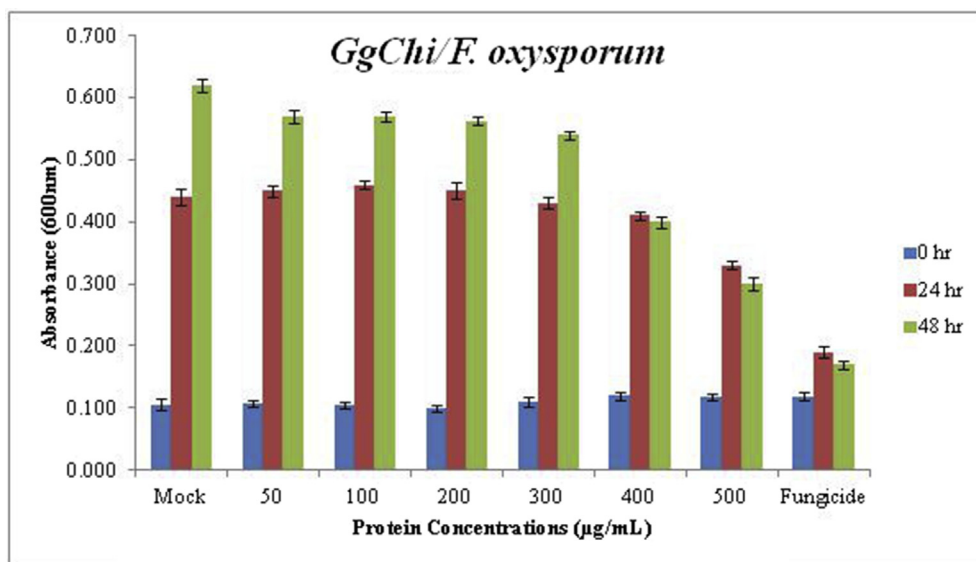


Figure 6. Antifungal activity of purified chitinase (GgChi) against *Fusarium oxysporum*. A mild antifungal activity was observed up till 400 µg/ml of the enzyme concentration in comparison to control in 24 h of the incubation. However, a decline in fungal growth started to appear after 48 h of the incubation at 400 and most notably at 500 µg/ml of GgChi. This concentration of 500 µg/ml resulted in 50% inhibition of the growth after 48 h of the incubation.

Table 3 GgChi showed moderate mortality against nymphs of *B. tabaci* as compare to control treatment.

Treatment	No. of Nymphs ^a	Adult Emergence	% Emergence	% Mortality	No. of Nymphs
GgChi	50	31	62	30	131
Control	50	38	76	23.2	151

^a Experiment was performed with five replicates and 10 nymphs per replicate.

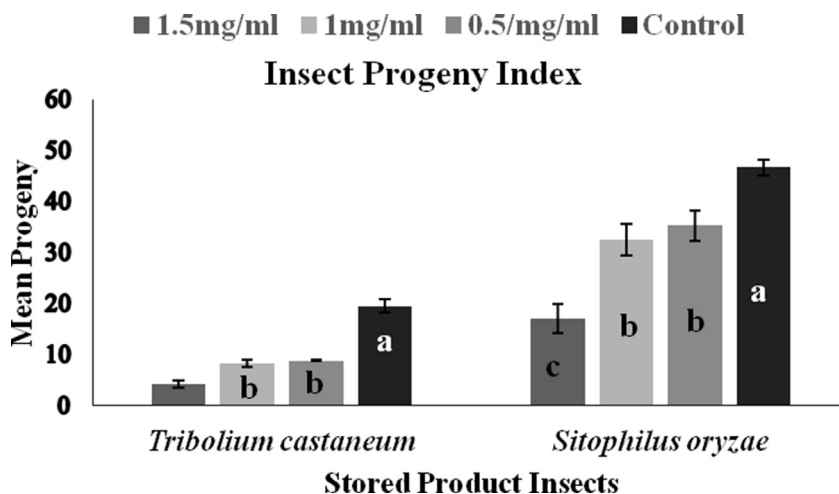


Figure 7. GgChi showed entomotoxicity against *T. castaneum* and *S. oryzae* progeny. GgChi (1.5 mg/ml) produced significant inhibition of *T. castaneum* and *S. oryzae* progeny in comparison to control.

enzymes from rice, no lytic or antifungal activity was reported for OsChib1a [36]. For the class III chitinase, GlcNAc specificity was reported only at subsite (-1), indicating that the target of the class III enzyme was not necessarily a consecutive GlcNAc sequence. It is possible that the class III rice chitinase might act toward GlcNAc-containing glycolipid or glycoprotein, producing or degrading the signal

molecules to control important biological processes other than pathogenesis. However, it is also known that chitin in the cell wall of mature hyphae is subjected to intensive modifications including deacetylation [37]. Chi18aC, chitinase from *S. coelicolor* which is most active toward crystalline chitin, did not show any significant antifungal activity. Chitinases have been thought to inhibit hyphal tip

extension when the newly synthesized chitin within the tips is not yet crystallized [38].

Plants released many toxic chemicals with antimicrobial activity as well as some toxicity to insect pests. In present study, chitinase showed some efficacy against the notorious insect species of stored commodities. *T. castaneum*; and *S. oryzae* progeny was reduced when compared to control set, which indicated the efficacy of chitinase higher in stored product insect pests than whitefly. Similarly, the effectiveness of chitinase extracted from latex of mulberry against larvae of common fruit fly (*Drosophila melanogaster*) has already been reported which supports the result of this experiment. It is suggested that chitinase protein hydrolyze the insect body which is made with chitin and this hydrolysis could result the protein towards its toxicity against insects [39]. So, entomo-toxic plant's molecules could be an appreciated approach to develop bio-insecticides against stored product insect pests.

Acknowledgements

We are thankful to the Institute of Food Science & Nutrition, Bahauddin Zakariya University Multan, Pakistan for help in absorbance readings and NARC, Islamabad, Pakistan for kind support in insecticidal activity assays.

References

- [1] Shahidi F, Abuzaytoun R. Chitin, chitosan, and co-products: chemistry, production, applications, and health effects. *Adv Food Nutr Res* 2005;49:93–135.
- [2] Hammami I, Siala R, Jridi M, Ktari N, Nasri M, Triki M. Partial purification and characterization of chiO8, a novel antifungal chitinase produced by *Bacillus cereus* IO8. *J Appl Microbiol* 2013;115:358–66.
- [3] Hamid R, Khan MA, Ahmad M, Ahmad MM, Abdin MZ, Musarrat J, et al. Chitinases: an update. *J Pharm BioAllied Sci* 2013;5:21.
- [4] Wang Q, Qu L, Zhang Z, Wang Y, Zhang Y. Characterization of a novel chitinase, DkChi, from *Dendrolimus kikuchii* nucleopolyhedrovirus. *Arch Virol* 2013;158:2523–30.
- [5] Salzer P, Bonanomi A, Beyer K, Vögeli-Lange R, Aeschbacher RA, Lange J, et al. Differential expression of eight chitinase genes in *Medicago truncatula* roots during mycorrhiza formation, nodulation, and pathogen infection. *Mol Plant Microbe Interact* 2000;13:763–77.
- [6] Kasprzewska A. Plant chitinases-regulation and function. *Cell Mol Biol Lett* 2003;8:809–24.
- [7] Tanabe T, Kawase T, Watanabe T, Uchida Y, Mitsutomi M. Purification and characterization of a 49-kDa chitinase from *Streptomyces griseus* HUT 6037. *J Biosci Bioeng* 2000;89:27–32.
- [8] Ohnuma T, Osawa T, Fukamizo T, Numata T. Crystallization and preliminary X-ray diffraction analysis of a class V chitinase from *Nicotiana tabacum*. *Acta Crystallogr Sect F Struct Biol Cryst Commun* 2010;66:1599–601.
- [9] Henrissat B, Bairoch A. New families in the classification of glycosyl hydrolases based on amino acid sequence similarities. *Biochem J* 1993;293:781–8.
- [10] Henrissat B, Davies G. Structural and sequence-based classification of glycoside hydrolases. *Curr Opin Struct Biol* 1997;7: 637–44.
- [11] Iseli B, Armand S, Boller T, Neuhaus J-M, Henrissat B. Plant chitinases use two different hydrolytic mechanisms. *FEBS Lett* 1996;382:186–8.
- [12] Wang H, Cui Y, Zhao C. Flavonoids of the genus *Iris* (*Iridaceae*). *Mini Rev Med Chem* 2010;10:643–61.
- [13] López RC, Gómez-Gómez L. Isolation of a new fungi and wound-induced chitinase class in corms of *Crocus sativus*. *Plant Physiol Biochem* 2009;47:426–34.
- [14] Han Y, Li Z, Miao X, Zhang F. Statistical optimization of medium components to improve the chitinase activity of *Streptomyces* sp. Da11 associated with the South China Sea sponge *Craniella australiensis*. *Process Biochem* 2008;43: 1088–93.
- [15] Kelley LA, Sternberg MJ. Protein structure prediction on the Web: a case study using the Phyre server. *Nat Protoc* 2009;4: 363–71.
- [16] Bradford MM. A rapid and sensitive method for the quantitation of microgram quantities of protein utilizing the principle of protein-dye binding. *Anal Biochem* 1976;72:248–54.
- [17] Laemmli UK. Cleavage of structural proteins during the assembly of the head of bacteriophage T4. *Nature* 1970;227: 680–5.
- [18] Menckhoff L, Mielke-Ehret N, Buck F, Vuletić M, Lüthje S. Plasma membrane-associated malate dehydrogenase of maize (*Zea mays* L.) roots: native versus recombinant protein. *J Proteom* 2013;80:66–77.
- [19] Murzin AG. Structural classification of proteins: new superfamilies. *Curr Opin Struct Biol* 1996;6:386–94.
- [20] Berman HM, Westbrook J, Feng Z, Gilliland G, Bhat TN, Weissig H, et al. The protein data bank. *Nucleic Acids Res* 2000;28:235–42.
- [21] Laskowski RA, MacArthur MW, Moss DS, Thornton JM. PROCHECK - a program to check the stereochemical quality of protein structures. *J Appl Crystallogr* 1993;26:283–91.
- [22] Pettersen EF, Goddard TD, Huang CC, Couch GS, Greenblatt DM, Meng EC, et al. UCSF Chimera—a visualization system for exploratory research and analysis. *J Comput Chem* 2004;25:1605–12.
- [23] Boyle VJ, Fancher ME, Ross RW. Rapid, modified Kirby-Bauer susceptibility test with single, high-concentration antimicrobial disks. *Antimicrob Agents Chemother* 1973;3:418–24.
- [24] Saleem M. Toxicological studies on synthetic pyrethroid against red flour beetle *Tribolium castaneum* (Herbst.) (Coleoptera: Tenebrionidae). Ph. D Thesis. University of Punjab; 1990.
- [25] Jaleel W, Saeed Q, Saeed S, Ansari T, Naqqash MN, Iqbal N, et al. Efficacy and time mortality of *Tribolium castaneum* (Herbst.) (Coleoptera: Tenebrionidae) by some essential oils through contact and fumigant methods. *Appl Sci Bus Econ* 2015;2:1–7.
- [26] Arthur FH. Susceptibility of last instar red flour beetles and confused flour beetles (Coleoptera: Tenebrionidae) to hydroperene. *J Econ Entomol* 2001;94:772–9.
- [27] Amin MA, Hameed A, Rizwan M, Akmal M. Effect of different insecticides against insect pests and predators complex on *Brassica napus* L. under field conditions. *Int J Sci Res Environ Sci* 2014;2:340.
- [28] Kuranda MJ, Robbins PW. Chitinase is required for cell separation during growth of *Saccharomyces cerevisiae*. *J Biol Chem* 1991;266:19758–67.
- [29] Watanabe T, Kobori K, Miyashita K, Fujii T, Sakai H, Uchida M, et al. Identification of glutamic acid 204 and aspartic acid 200 in chitinase A1 of *Bacillus circulans* WL-12 as essential residues for chitinase activity. *J Biol Chem* 1993;268: 18567–72.
- [30] Busby JN, Landsberg MJ, Simpson RM, Jones SA, Hankamer B, Hurst MR, et al. Structural analysis of Chi1 chitinase from *Yersinia entomophaga*. *J Mol Biol* 2012;415:359–71.
- [31] Synstad B, Gåseidnes S, Van Aalten DM, Vriend G, Nielsen JE, Eijsink VG. Mutational and computational analysis of the role

- of conserved residues in the active site of a family 18 chitinase. *Eur J Biochem* 2004;271:253–62.
- [32] Taira T, Noriko T, Ishihara M. Purification, characterization, and antifungal activity of chitinases from pineapple (*Ananas comosus*) leaf. *Biosci Biotechnol Biochem* 2005;69:189–96.
- [33] Lu Z-X, Laroche A, Huang HC. Isolation and characterization of chitinases from *Verticillium lecanii*. *Can J Microbiol* 2005;51:1045–55.
- [34] Boot RG, Blommaert EF, Swart E, Ghauharali-van der Vlugt K, Bijl N, Moe C, et al. Identification of a novel acidic mammalian chitinase distinct from chitotriosidase. *J Biol Chem* 2001;276:6770–8.
- [35] Vogelsang R, Barz W. Purification, characterization and differential hormonal regulation of a β -1, 3-glucanase and two chitinases from chickpea (*Cicer arietinum* L.). *Planta* 1993;189:60–9.
- [36] Sasaki C, Yokoyama A, Itoh Y, Hashimoto M, Watanabe T, Fukamizo T. Comparative study of the reaction mechanism of family 18 chitinases from plants and microbes. *J Biochem* 2002;131:557–64.
- [37] Ruiz-Herrera J, Martinez-Espinoza AD. Chitin biosynthesis and structural organization in vivo. *Exs* 1998;87:39–53.
- [38] Kawase T, Yokokawa S, Saito A, Fujii T, Nikaidou N, Miyashita K, et al. Comparison of enzymatic and antifungal properties between family 18 and 19 chitinases from *S. coelicolor* A3 (2). *Biosci Biotechnol Biochem* 2006;70:988–98.
- [39] Kitajima S, Kamei K, Taketani S, Yamaguchi M, Kawai F, Komatsu A, et al. Two chitinase-like proteins abundantly accumulated in latex of mulberry show insecticidal activity. *BMC Biochem* 2010;11:6.